SCS&E Report 9315
November, 1993

Two-dimensional Numerical Simulations of High-efficiency Silicon Solar Cells

Gernot Heiser, Armin G. Aberle, Stuart R. Wenham, Martin A. Green

(The text of this report will also appear in the Microelectronics Journal)

SCHOOL OF COMPUTER SCIENCE AND ENGINEERING
THE UNIVERSITY OF NEW SOUTH WALES

Abstract

This paper reports on the first use of two-dimensional (2D) device simulation for optimising the front-finger spacing of one-sun high-efficiency silicon solar cells of *practical* dimensions. We examine the 2D current flow patterns in these devices under various illumination conditions, resulting in improved insight into the operating conditions of the cells. Results for the optimal spacing of the front metal fingers are presented and compared to predictions obtained from 1D simulations. We also address difficulties facing the numerical modelling of high-efficiency silicon solar cells.

1 Introduction

Solar cells directly convert sunlight into electricity without polluting by-products and represent a promising, environmentally attractive technology to cover the world's future energy needs. Today, most terrestrial solar cells are made from silicon (Si). This has the advantage of using a raw material that is cheap, abundant and non-toxic, and there is the benefit of three decades of extensive experience in processing the material. The disadvantages of Si are lower theoretical efficiencies, compared to cells based on gallium arsenide, and the fact that long wavelength light is only weakly absorbed in Si, which requires relatively thick devices. However, the incorporation of elaborate light-trapping schemes into Si solar cells of reduced thickness (thin-film technologies) make Si a promising candidate for future cost-effective solar cells.

To improve the competitiveness of solar cells as a source of electrical energy, their efficiency must be increased. The last decade saw enormous progress in Si solar cell efficiency, culminating in the demonstration of a 23.1 % efficient monocrystalline one-sun cell made at the University of New South Wales (UNSW) [1, 2], and a concentrator solar cell made at Stanford University, reaching about 27 % conversion efficiency at 200 suns [1, 3]. Further significant improvement is possible, as the technological limit of Si cells under non-concentrated solar illumination is about 29 %.

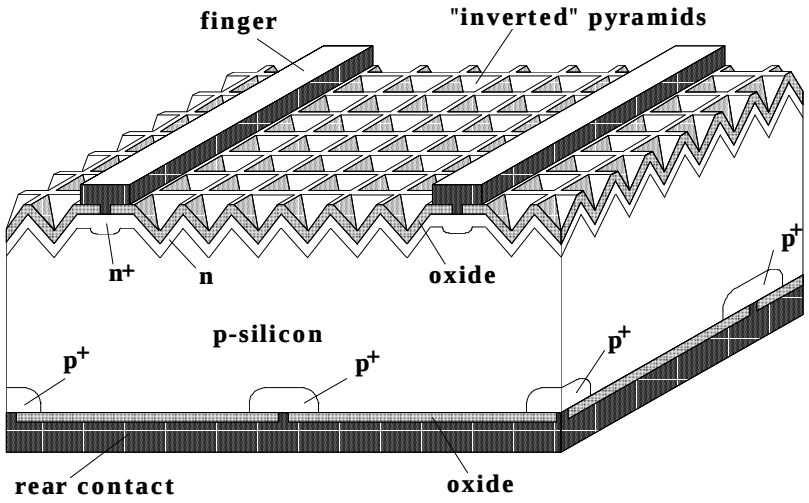

Figure 1: The UNSW PERL Si solar cell [2].

Fig. 1 shows the "passivated emitter, rear locally-diffused" (PERL) cell recently developed at UNSW, which presently represents the best trade-off between various factors limiting Si cell efficiency under one-sun illumination. It is estimated that PERL cells can yield efficiencies of up to 25 % if all design parameters are fully optimised. However, this requires improved insight into the operating conditions of the devices. Numerical modelling is an excellent means to gain such improved insight, as it allows the observation of variables that are impossible or very difficult to measure.

In this paper we report on the first use of two-dimensional (2D) numerical simulations for the optimization of the front finger spacing of one-sun high-efficiency Si solar cells of *realistic* dimensions. In the past, 2D simulations of silicon solar cells have been undertaken, e.g. by Gray et al. [4], using SCAP2D, and Ghannam et al. [5], using Pisces. However, a comprehensive treatment of 2D effects in high-efficiency Si solar cells has not yet been published. At UNSW, we have started a project aiming at an improved understanding of the operating conditions of these devices by using two- and three-dimensional numerical modelling. The recently developed device simulation package *Simul* [6] from ETH-Zurich is well-suited to such investigations. Simul uses a grid generator that provides precise control over

the grid density while avoiding certain numerical problems resulting from meshes containing obtuse triangles [7]. The package has recently been extended to photovoltaic applications by the inclusion of optical generation [8] and is particularly suited to the simulation of large-area devices such as solar cells.

The remainder of this paper is structured as follows: Section 2 briefly summarises the basic operation principles and limitations of Si solar cells and qualitatively discusses the 2D effects arising from the design of the front electrode. In Section 3, the numerical difficulties and limitations in the modelling of these devices are outlined. Section 4 presents and discusses the current flow patterns at one-sun maximum power point conditions for various illumination spectra and shows the dependence of the cell output on the front finger spacing.

2 Silicon Solar Cells

The basic principle of solar cell operation is the generation of an electron-hole pair by the absorption of a photon and the subsequent spatial separation of the carriers by means of a built-in electric field. In most practical solar cells the built-in field is created by means of a p-n junction. For highest cell efficiency, an optimal trade-off between optical and electrical (i.e. ohmic and recombinative) losses needs to be determined.

The major reason for the relatively low maximum efficiency of Si solar cells (around 29 % at one-sun illumination) is related to the bandap of Si (1.12eV) and the fact that each photon, regardless of its energy, can only create a single e-h pair. Thus, light of wavelengths above 1.11μm is not absorbed by Si, while for shorter wavelengths the photon energy exceeding 1.12eV is converted to heat and therefore lost for electricity production. This limits the maximum short-circuit current, J_{sc}, to about 44mA/cm^2 under solar illumination at the earth's surface (AM1.5 spectrum). The second limitation relates to the maximum output voltage (open-circuit voltage, V_{oc}), which cannot be greater than the built-in potential drop across the p-n junction (i.e. $\approx$ 0.9V, compared to the 1.12V of the bandgap). Finally, the I-V curve of the cell is not rectangular but exponential, so that the maximum power output is further reduced by the *fill factor*,

$$FF = \frac{J_{mpp} V_{mpp}}{J_{sc} V_{oc}}, \tag{1}$$

where J_{mpp}, V_{mpp} are the current and voltage, respectively, at the "maximum power point" (MPP) of the cell. The theoretical limit for FF of silicon solar cells is 0.9 [11].

Further losses in real devices arise from recombination losses (bulk, surfaces, metal contacts), shading losses at the metal contacts, reflection losses, and resistive losses (semiconductor and contacts). These limit the cell efficiency to the above-mentioned value of about 29 % under one-sun illumination [9, 10, 11].

In the case of *conventional* n^+p solar cells (i.e. cells with bifacial metal contacts and a full-area current-collecting n^+ "emitter" along the illuminated front surface) the front electrode consists of a comb-like metal grid. A critical parameter of this cell structure is the spacing of the front metal fingers. Since metal contacts are opaque to light, closely spaced fingers lead to high shading losses. On the other hand, for widely spaced front fingers, ohmic losses associated with the lateral flow of majority carriers in the emitter degrade the cell's efficiency.

Many of the high-efficiency features of present Si solar cells, e.g. the optimum doping profile below oxidised and metallised Si surfaces, resulted from one-dimensional computer simulations. However, current flow in modern cells deviates strongly from a simple one-dimensional model. This is indicated in Fig. 2 for the flow of electrons in a simplified n^+p solar cell. This cell differs from the PERL cell by having a flat surface and a fully metallised back.

As the Figure indicates, electrons generated within the emitter will flow horizontally towards a front metal finger, electrons created near the junction in the "base" (i.e. the p layer of the n^+p diode) will first diffuse vertically across the junction. The horizontal flow of electrons through the emitter will result in a voltage drop, and hence the central emitter region is at a lower potential than the vicinity of the

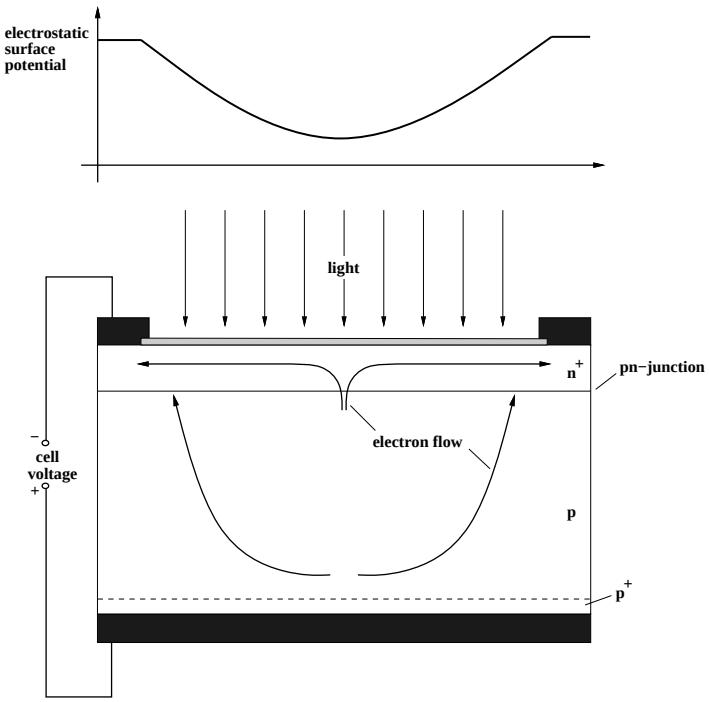

Figure 2: Electrostatic potential at the emitter surface (above) and (below) the lateral electron current flow in the emitter and the base of a uniformly illuminated n^+pp^+ Si solar cell.

contacts. This voltage drop leads to a higher forward injection of carriers from the central emitter region and hence to an increased concentration of minority carriers in the top central base region compared to near the contacts. This effect is enhanced by the lack of photo-generation under the opaque contacts. As minority carrier motion is controlled by diffusion (rather than drift) under low injection conditions, this concentration gradient in the base leads to electron trajectories that deviate strongly from simple straight lines, ultimately a consequence of the large distance between the metal contacts at the front of the cell.

The most sophisticated modelling approach based on one-dimensional (1D) theory is schematically shown in Fig. 3 [12]. The solar cell is modelled by two separate diodes, an illuminated and a dark one. Obviously, this 1D model cannot take into account effects arising due to lateral electron flow in the base.

3 Numerical Modelling of Si Solar Cells: Difficulties and Limitations

One important design parameter of conventional Si solar cells is the *front contact spacing*, i.e. the distance between the thin metal fingers contacting the emitter layer. Since 1D models assume a purely vertical electron flow in the base they overestimate the current flow in the emitter, and hence the ohmic losses. It can therefore be expected that a proper numerical treatment will result in a larger value for the optimal distance between front contact fingers than what is predicted by a 1D treatment.

The PERL cell of Fig. 1 is a three-dimensional (3D) structure, and proper modelling of all of its features would require 3D simulations. However, in this paper we are mainly concerned with effects arising from the finite resistance of the emitter layer and its effect on the optimal spacing of the front contact fingers. Since the PERL cell operates in low injection at one-sun illumination, the point-like back contacts have little influence on the electron current flow in the cell. We therefore replaced in all our simulations the point-like back contacts by a fully metallised back with a p^+ "back surface field".

Furthermore we ignored the texture (i.e. the inverted pyramids) of the front surface. The rationale is

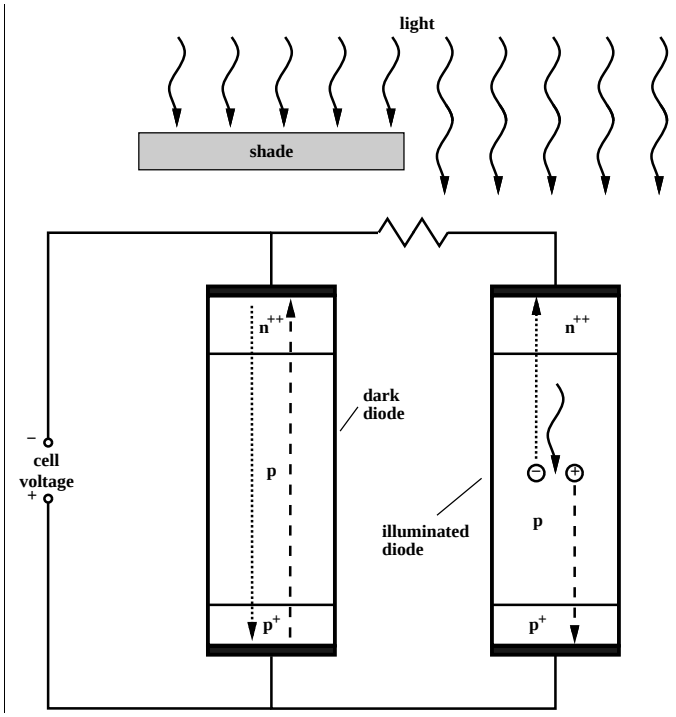

Figure 3: Solar cell modelling based on 1D theory: The cell is considered to consist of two parallel diodes, an illuminated and a dark one. The resistor accounts for ohmic losses in the emitter.

that the relatively small pyramids ($10\mu\mathrm{m} \times 10\mu$m squares, 7μm deep) do not have a significant effect on the overall current flow pattern; the textured emitter can therefore be replaced by a flat emitter with an appropriate sheet resistivity. Of course, the surface texture has an enormous effect on reflection losses; we allow for this by adjusting the intensity of the incoming light so that we obtain an J_{sc} value of around 40mA/cm^2, which is typical for one-sun high-efficiency silicon solar cells. This leads to the solar cell structure of Fig. 2, with the added benefit that the results are not specific to PERL cells but apply to conventional high-efficiency one-sun Si solar cells in general.

Even under these simplifying assumptions high-efficiency Si solar cells are notoriously difficult to simulate. The main reason is that these cells combine microscopic features with macroscopic dimensions, as indicated in Fig. 4. Symmetry arguments allow reduction of the full cell to an irreducible simulation domain limited by the center of a contact finger at one side (the left in Fig. 4) and the mid-point between two contact fingers at the other side. The full depth of the cell must be simulated, as the whole volume is electronically active.

In order to perform numerical modelling of such a device, it is essential that all the (microscopic) device features are properly resolved. This means that the thin emitter needs to be resolved by points spaced at most about 0.1μm apart in the y-direction (i.e. vertically), that the shadow boundary (across which the generation rate is discontinuous) needs similar resolution in the x-direction, and that a point spacing of at most 1μm is required in the y-direction to resolve the somewhat deeper p^+ "back surface field" near the base contact. In addition, the highly doped region under the emitter contact needs to be resolved. Obviously a strong variation of the grid density throughout the device is required, as a regular grid that resolves the above features would contain about a million grid points, too much to be usable even on big supercomputers. A typical grid as used in our simulations is shown in Fig. 5. The refinement of the areas mentioned above can clearly be seen. Fig. 6 shows a magnification of the left upper corner of Fig. 5, i.e. the vicinity of the emitter contact, showing the strong variation of the grid point density.

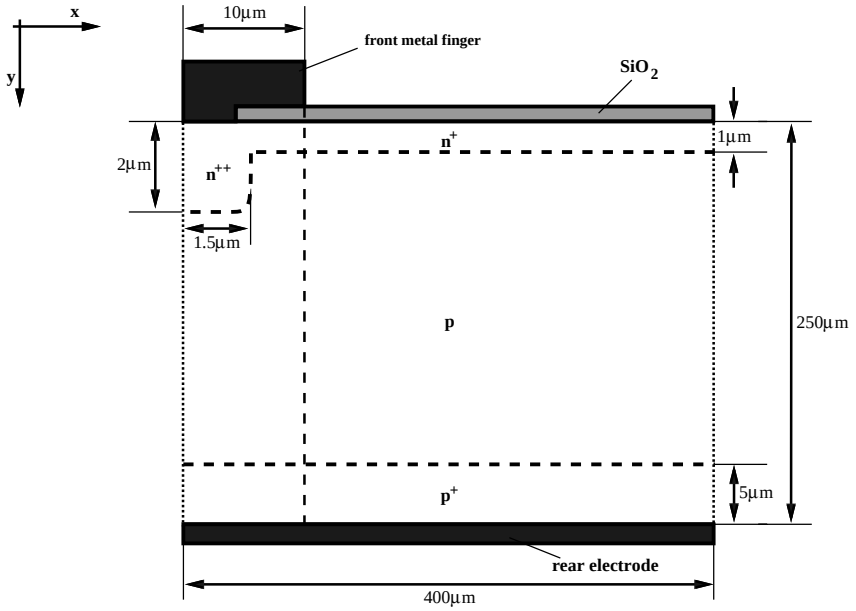

Figure 4: Typical dimensions of the irreducible section of a high-efficiency Si solar cell.

The Figure also shows the doping profile in the region.

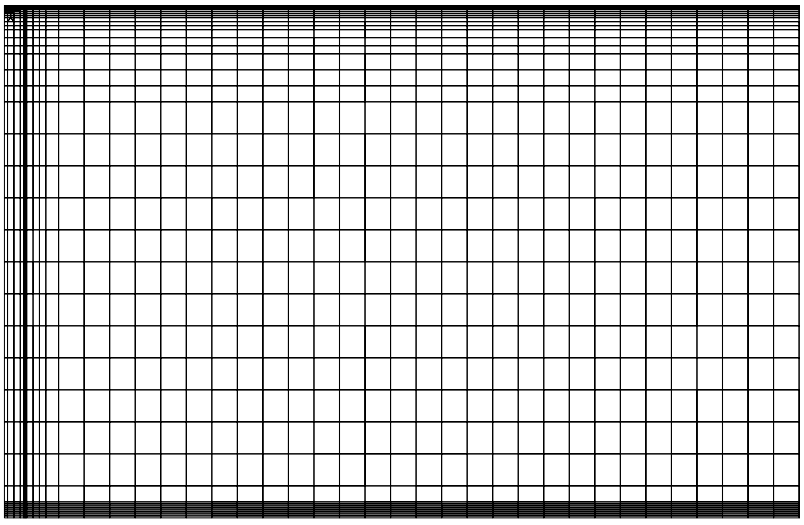

Figure 5: Typical simulation grid used in this study. This grid contains 2935 points, the simulation domain is 400μm wide and 250μm deep.

The optical generation rates in the cell are shown in Fig. 7. The black region at the left is the part of the cell shaded by the front contact. It can be seen that in most of the base the generation rate varies by less than an order of magnitude. This is a result of the weak absorption of long wavelengths in Si, about half of the light is already absorbed in the emitter, and at depths exceeding 10μm only the longest wavelengths survive.

The situation is quite different in the emitter; the optical generation rate is about four orders of

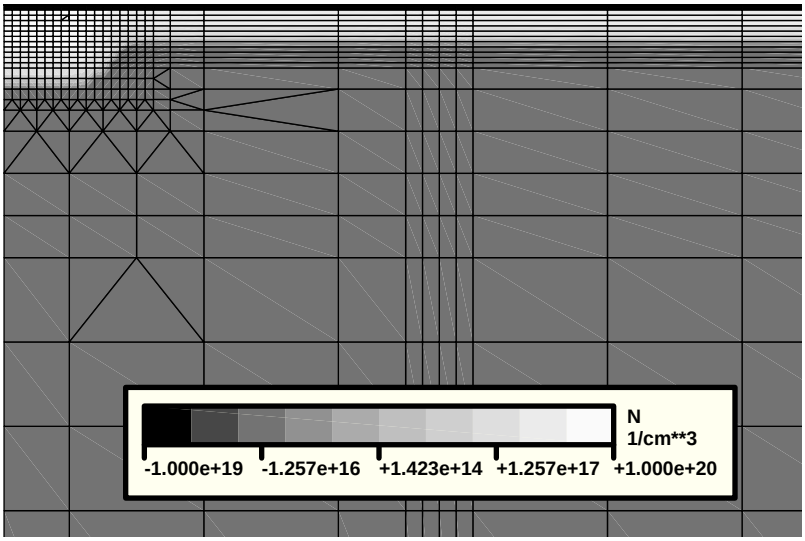

Figure 6: Simulation grid and doping concentration near the emitter contact. Light colours indicate n-doping, dark colours p-doping. The area shown is about 17μm wide and 12μm deep.

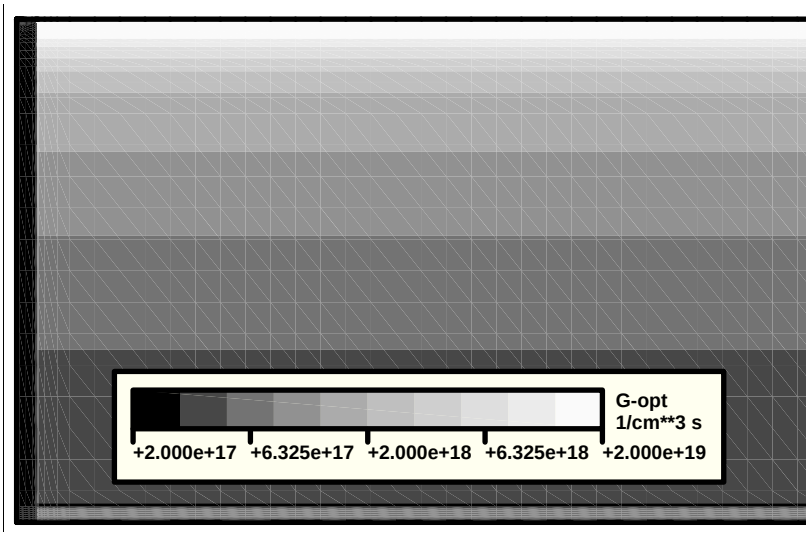

Figure 7: Rate of optical carrier generation in the cell.

magnitude larger at the front of the cell than at the back. Due to the strong absorption, short wavelength light does not penetrate very deep into the Si and there is an exponential decay of generation rates within the top portion emitter, as shown in Fig. 8. Within the top 0.1μm the optical generation rate drops by a factor of 4. In order to properly determine surface recombination losses, an extremely dense grid is required to properly model carrier generation near the front surface. The grid we use has points spaced in the y-direction as close as one nanometer at the front surface. To avoid obtaining an excessive number of points, the grid elements (rectangles) near the top surface have aspect ratios exceeding 10,000.

Solar cells (and hence solar cell simulations) are extremely sensitive to all factors determining the concentration of minority carriers, such as recombination mechanisms and the value of the *intrinsic*

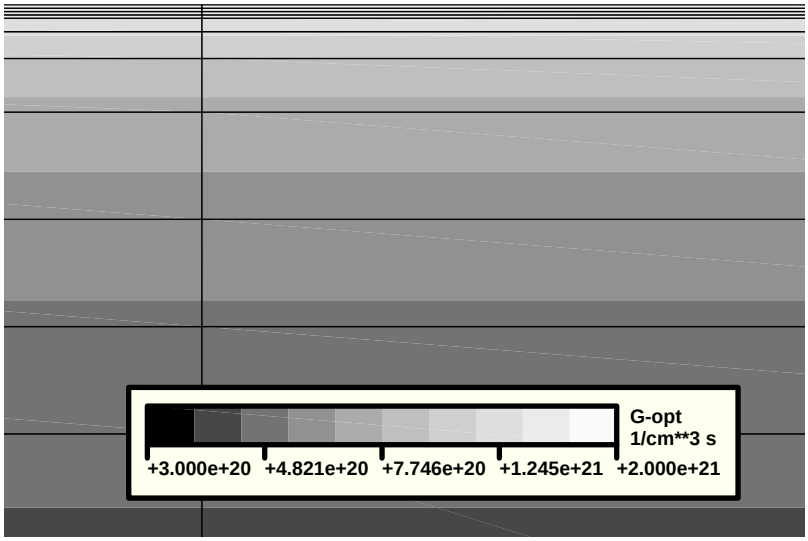

Figure 8: Optical generation rate and simulation grid in the top 0.15μm of the emitter.

carrier concentration, n_i. The latter is the concentration of electrons and holes in undoped Si and its exact value has an important effect on the minority carrier concentration in doped material. To account for an apparent narrowing of the bandgap at high dopant concentrations, an *effective intrinsic carrier concentration*, n_{ie}, is used in device simulators. Several models for n_{ie} are in use, each resulting in a different value of n_i. Table 1 shows how the four models available in Simul result in different simulated power output under otherwise identical conditions.

n_{ie} model	oS	S	dA	BW	BW*
$n_i[10^{10}\,\mathrm{cm}^{-3}]$	1.548	1.247	1.493	1.09	1.00
$P/P_{\mathrm{BW}*}$	0.804	0.885	0.934	0.994	1.000

Table 1: Simulated power output using different models of the effective intrinsic density, n_{ie}. The models "oS" (oldSlotboom), "S" (Slotboom), "dA" (delAlamo), and "BW" (Bennett-Wilson) are as implemented in Simul using default parameters, "BW*" is the BW model modified to yield a value of $n_i = 1.0 \times 10^{10}\mathrm{cm}^{-3}$, which is the value currently accepted in the photovoltaic community [13].

The computed cell output shows similar sensitivities to other models determining the minority carrier concentration, in particular recombination models. It is obvious that under these circumstances a comparison of simulated and measured cell efficiencies is rather problematic. We have therefore made no attempt to simulate absolute efficiencies, instead we have adjusted the light intensity such that a typical value of J_{sc} is obtained and only performed relative comparisons of cell output.

4 Results

Fig. 9 shows typical current and power characteristics of the investigated Si solar cell. The maximum power point is at a bias of 590mV and the fill factor is 83.6 %. Such a simulation with a grid of about 3000 points typically ran for about 1.5 hours on a Sun SPARCclassic workstation or about 10 minutes on a Fujitsu VP-2200 supercomputer. Memory usage was of the order of 15Mbytes. The linear systems

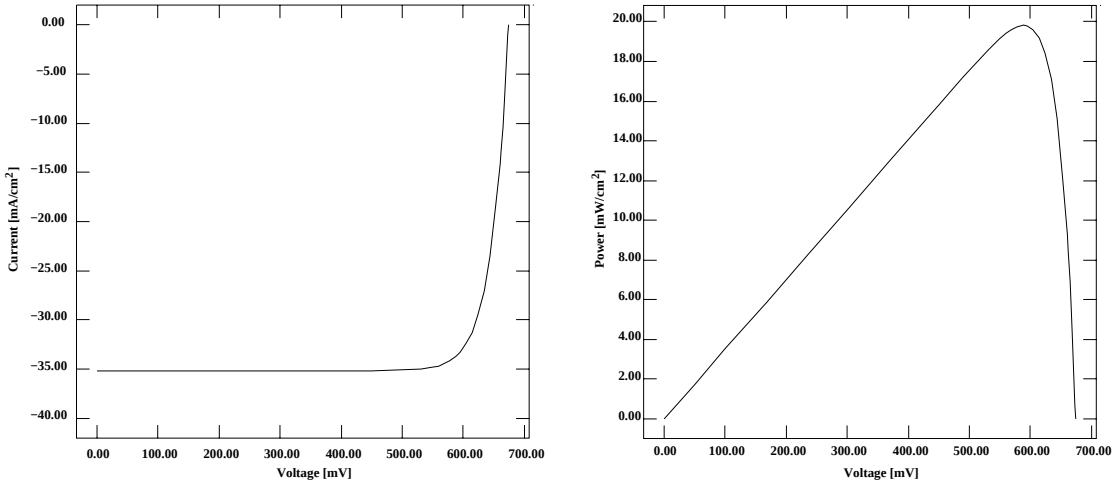

Figure 9: I-V (left) and P-V (right) characteristics of a typical high-efficiency Si solar cell under AM1.5 illumination.

were solved by the *CGSTAB* method preconditioned with an incomplete factorisation based on numerical dropping [14].

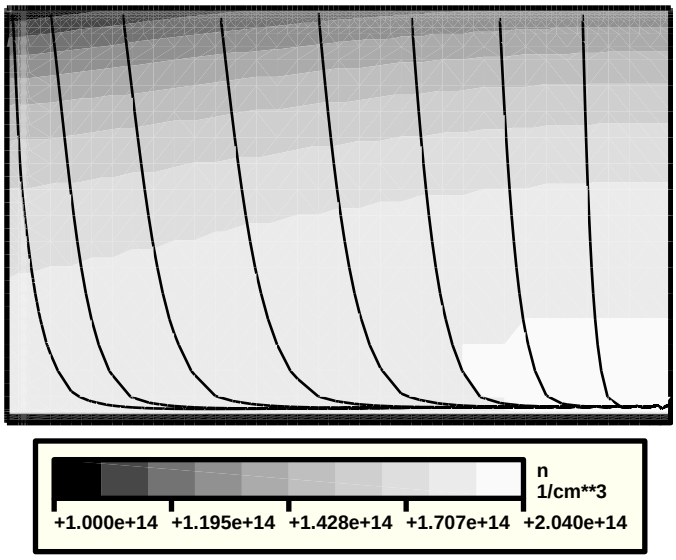

Figure 10: Electron density at MPP in a solar cell with a front contact spacing of 800μm illuminated with light of 1000nm wavelength of an intensity corresponding to one sun. The black lines indicate the direction of current flow.

Fig. 10 shows the electron density and electron trajectories at MPP in the base of a cell with finger spacing of 800μm (i.e. a simulation domain of 400μm width). In this simulation the cell is illuminated with near-infrared light (of an intensity corresponding to one sun) and operates at maximum power point conditions. Near the rear surface the electron flow is strongly 2D. Electrons generated near the back move a considerable distance along the rear surface until they diffuse upwards to be collected by the p-n junction. It can be expected that the 2D effect increases if the finger spacing becomes larger. Fig. 11 confirms this for a cell with double the finger spacing of Fig. 10.

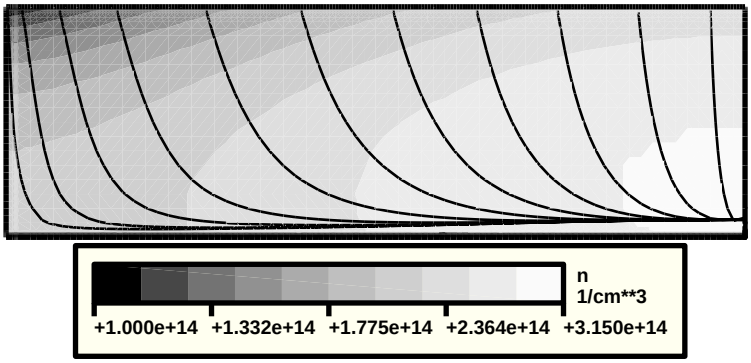

Figure 11: Electron density and flow lines at MPP in a solar cell under one-sun illumination with 1000nm wavelength. The front contact spacing is 1600μm.

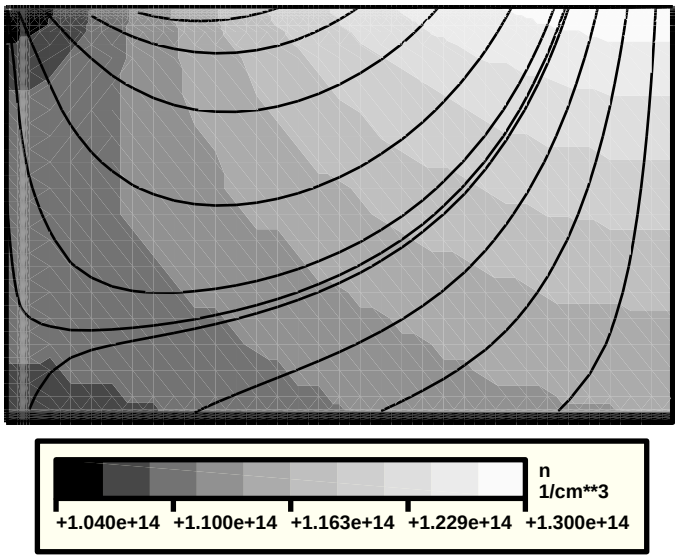

Figure 12: Electron density and flow lines at MPP in a solar cell under one-sun illumination with 400nm wavelength. The front contact spacing is 800μm.

Illumination with short-wavelength light results in a completely different picture: Fig. 12 shows the cell of Fig. 10 illuminated with blue light. As explained earlier, such light is completely absorbed within the top 0.1μm of the emitter. However, it can be seen that the base is not completely inactive as far as electrons are concerned: the electron flow within the emitter creates a voltage drop along the front surface. As discussed in Section 2, this voltage profile leads to a forward injection of electrons into the base. The injected current corresponds to several percent of the light-generated electrons. Upon entering the base, about 1/4 of these electrons diffuse towards the rear surface before recombining. The remainder, however, is redirected and eventually collected by the p-n junction in the vicinity of the front metal finger.

Fig. 13 shows the corresponding electron density and the direction of the electron flow under AM1.5 (i.e. white) illumination. Here, the effects of strong absorption at short wavelengths and weak absorption at long wavelengths combine to produce a maximum of the electron density at a depth of about 25μm,

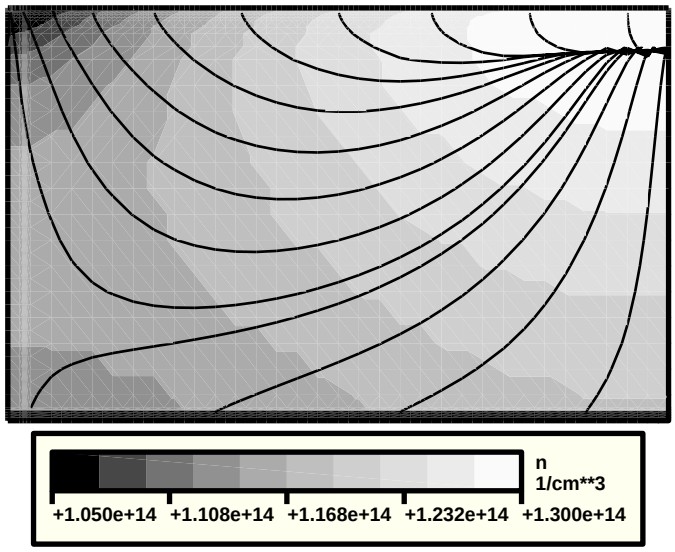

Figure 13: Electron density and flow lines at MPP in a solar cell with finger spacing of 800μm under AM1.5 illumination.

i.e. in the top region of the base but still well below the emitter. The result is an electron flow which, in most of the device, is more horizontal than vertical. Consequently, a significant fraction of the electron current that otherwise would have to be transported by the emitter flows through the base of the cell. This effect reduces the current density and hence the ohmic losses in the emitter. However, due to the enhanced electron path length in the base, this 2D effect is only beneficial for solar cell efficiency if the electron diffusion length is larger than about half the front finger spacing. This condition is satisifed for UNSW cells which feature a diffusion length of 1–2mm for electrons.

In Fig. 14, the impact of the 2D effects on the cell performance is calculated as a function of the front finger spacing. As expected, the 2D simulations predict a larger finger spacing than the 1D simulations. However, at one-sun illumination, the difference is rather small: 1.2mm compared to about 1.0mm. It can therefore be said that in spite of the strong deviations from 1D current flow, the predictions of 1D simulations for the optimum front finger spacing is surprisingly good. It should be noted that both models predict an optimum finger spacing which is larger than the value of 0.8mm presently used in the UNSW cells.

With increasing light intensity, due to the larger lateral emitter currents, the 2D effects in the base become more pronounced. We have shown elsewhere [15] that this leads to an increasing discrepancy between 1D and 2D results.

5 Conclusions and Future Work

The 2D simulations presented in this paper show that current flow in conventional high-efficiency Si solar cells deviates strongly from what is assumed by 1D models. Parameter studies aimed at optimizing an important design parameter, the front finger spacing, have been performed and an improved value for the front finger spacing for one-sun cells has been obtained. Masks are presently being prepared to test the new design rule. It has also been found that for non-concentrated sunlight 1D simulations can still provide reasonable predictions of the optimal front finger spacing.

Optimization studies of the back contact geometry of PERL cells using 2D and 3D simulations are presently under way, first results of 2D simulations have been submitted for publication [16, 17]. We

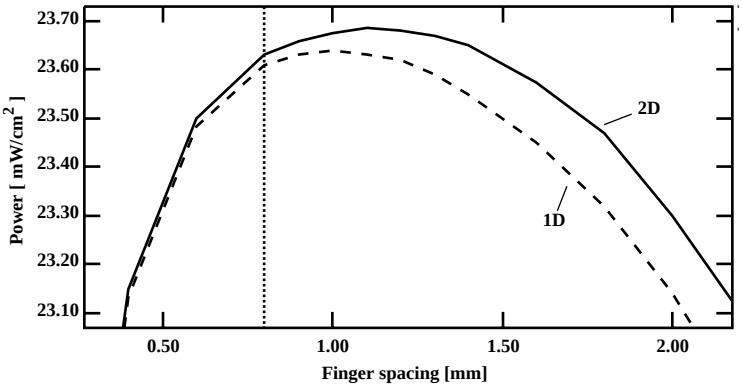

Figure 14: Comparison of 1D and 2D results for the dependence of the one-sun cell output on the spacing of the front contact fingers. The dotted line indicates the value of 0.8mm presently used in UNSW PERL cells.

are also investigating alternative cell designs allowing for superiour cell efficiencies.

6 Acknowledgments

This work was partially funded by a grant from the Australian Research Council (ARC) and a supercomputer grant from the Australian Institute for Nuclear Science and Engineering. The Centre for Photovoltaic Devices and Systems is supported by the ARC's Special Research Centres Scheme and Pacific Power. A.G.A. gratefully acknowledges the support of a Feodor Lynen Fellowship provided by the German Alexander von Humboldt Foundation. We like to thank Wolfgang Fichtner from ETH Zürich for granting access to the latest versions of Simul and Kevin Kells and Ulrich Krumbein of his group for their help with various problems encountered in the simulations. Finally, we would like to thank Frank Crawford from Australian Numerical Simulation and Modelling Services for his enthusiastic support when porting Simul to the Fujitsu VP-2200 supercomputer.

This is an extended version of a paper presented at the 5th International Conference on Simulation of Semiconductor Devices and Processes held in Vienna in September 1993.

References

[1] M. A. Green and K. Emery. Solar cell efficiency tables. *Progress in Photovoltaics*, 1:25–9, 1993.

[2] A. Wang, J. Zhao, and M. A. Green. 24 % efficient silicon solar cells. *Journal of Applied Physics Letters*, 57:602, 1990.

[3] R. Sinton, Y. Kwark, J. Gan, and R. Swanson. 27.5 % silicon concentrator solar cells. *IEEE Transactions on Electron Devices Letters*, 7:567, 1986.

[4] J. Gray, R. Schwartz, and R. Nasby. Two dimensional effects in conventional solar cells operated at high intensities. In *International Electron Devices Meeting*, pages 107–10. IEEE, 1982.

[5] M. Ghannam, E. Demesmaeker, J. Nijs, R. Mertens, and R. Van Overstraeten. Two dimensional study of alternative back surface passivation methods for high-efficiency silicon solar cells. In *Proceedings of the 11th European Communities Photovoltaic Solar Energy Conference*, pages 45–8, Montreux, Switzerland, October 1992.

[6] Integrated Systems Lab. *Simul Manual*. ETH Zürich, Switzerland, 1992.

[7] S. Müller, K. Kells, and W. Fichtner. Automatic rectangle-based adaptive mesh generation without obtuse angles. *IEEE Transactions on CAD ICAS*, CAD-11:855–63, 1992.

[8] U. Krumbein and W. Fichtner. Numerical simulation of optical carrier generation. Technical Report 91/22, Integrated Systems Laboratory, 1991.

[9] S. M. Sze. *Physics of Semiconductor Devices*. John Wiley, 2nd edition, 1981.

[10] A. L. Fahrenbruch and R. H. Bube. *Fundamentals of Solar Cells*. Academic Press, 1983.

[11] M. A. Green. *Solar Cells*. Prentice-Hall, 1982.

[12] A. G. Aberle, W. Warta, J. Knobloch, and B. Voss. Surface passivation of high efficiency silicon solar cells. In *Proceedings of the 21st IEEE Photovoltaic Specialists Conference*, page 233, Orlando, USA, 1990.

[13] A. B. Sproul and M. A. Green. Improved value for the silicon intrinsic carrier concentration from 275 to 375 K. *Journal of Applied Physics*, 70:846–54, 1991.

[14] C. Pommerell and W. Fichtner. Memory aspects and performance of iterative solvers. In *Copper Mountain Conference on Iterative Methods, Preliminary Proceedings*. SIAM, 1992. To appear in SIAM Journal on Scientific Computing, 1994.

[15] A. G. Aberle, S. R. Wenham, M. A. Green, and G. Heiser. Decreased emitter sheet resistivity loss in high efficiency silicon solar cells. *Progress in Photovoltaics*, 2, January 1994.

[16] G. Heiser and A. G. Aberle. Numerical modeling of non-ideal current-voltage characteristics of high-efficiency silicon solar cells. Submitted to *NUPAD-V*, October 1993.

[17] A. G. Aberle, M. A. Green, and G. Heiser. Two-dimensional numerical optimisation study of the rear point-contact geometry of high-efficiency silicon solar cells. Submitted to *Journal of Applied Physics*, October 1993.